An ultramarine fluorescent protein

with increased photostability and pH insensitivity

Wataru Tomosugi[1], Tomoki Matsuda[1], Tomomi Tani[1], Tomomi Nemoto[2], Ippei Kotera[1], Kenta Saito[3], Kazuki Horikawa[3] and Takeharu Nagai[1,3]

[1] Laboratory for Nanosystems Physiology, Research Institute for Electronic Science, Hokkaido University, N20 W10 Kita-ku, Sapporo, Hokkaido 001-0020, Japan

[2]Supportive Center for Brain Research, National Institute for Physiological Science, 38 Nishigonaka, Okazaki, Aichi 444-8585, Japan

[3]Nikon imaging center, Research Institute for Electronic Science, Hokkaido University, N20 W10 Kita-ku, Sapporo, Hokkaido 001-0020, Japan

¶Correspondence should be addressed to T.N.

tnagai@es.hokudai.ac.jp

tel +81-11-706-9438

fax +81-11-706-9443

Abstract

We report a pH-insensitive and photostable ultramarine fluorescent protein, Sirius, with an emission peak at 424 nm, the shortest emission wavelength among fluorescent proteins reported to date. The pH-insensitivity of Sirius allows prolonged visualization of biological events in an acidic environment. Furthermore, two FRET (fluorescence resonance energy transfer) pairs, Sirius-mseCFP and Sapphire-DsRed, allow dual-FRET imaging with single wavelength excitation, enabling detection of Ca^{2+} concentration and caspase-3 activation in the same apoptotic cells.

Among the fluorescent proteins reported to date, the variant with a Phe66 mutation in wild type green fluorescent protein (FP) from *Aequorea Victoria* exhibits the shortest emission wavelength, peaking at 442 nm[1]. However, fluorescence quantum yield of the Phe66 variant is low (Φ_{FL}= 0.013), strictly limiting its applicability for bioimaging.

To evolve the dim Phe66 mutant into a bright fluorescent protein, we carried out random mutagenesis on the sequence encoding four amino acids surrounding the chromophore of mseCFP-W66F, which was made by introducing the W66F mutation into the cyan FP variant, mseCFP[2] (**Table 1** and **Supplementary Fig. 1**). Four substitutions (T65Q, Y145G, H148S, and T203V: **Supplementary Fig. 1**) resulted in an ultramarine FP with 25-fold increase in fluorescence intensity (**Fig. 1a** and **Supplementary Fig. 2**). This protein, UMFP-1, showed an emission peak at 424 nm and a bimodal absorption peak at 280 and 355 nm (**Fig. 1b**). Owing to its greatly blue-shifted spectrum, UMFP-1 is spectrally compatible for multi-color imaging with CFP, YFP (yellow FP) and RFP (red FP) (**Fig. 1c-g**) In addition, UMFP-1 could be used in an extra detection channel distinct from BFP (blue FP) for extended multicolor imaging, by conducting linear spectral unmixing (**Supplementary Fig. 3**).

To improve the brightness of UMFP-1 further, we introduced an F46L mutation into the protein, yielding UMFP-2; this mutation promotes chromophore maturation at 37 ^{o}C [3]. Then, we conducted two more rounds of random mutagenesis on the entire gene using

error-prone PCR, and obtained still-brighter mutants UMFP-3 (UMFP-2-Q69L) and UMFP-4 (UMFP-3-F223S) (**Supplementary Fig. 1**). The final variant UMFP-4, which we re-named "Sirius" after a bright blue star in Canis Major, showed 80-fold brighter fluorescence than mseCFP-W66F, while retaining the same spectrum as UMFP-1 (**Table 1** and **Supplementary Fig. 2**). These increases in fluorescence intensity were mainly due to improvements in Φ_{FL} (**Table 1**).

To our surprise, although Sirius had a smaller absorption coefficient (ε) and Φ_{FL} than the BFPs, its fluorescence intensity in bacterial cells at 37 ^{o}C was about twice that of EBFP and 2/3 of EBFP2 (**Supplementary Fig. 4a**). We also observed a similar fluorescence intensity in mammalian cells (**Supplementary Fig. 4b**), suggesting that the Sirius chromophore underwent efficient posttranslational maturation in the intracellular environment at 37 ^{o}C. Concordantly, Sirius's rate of chromophore oxidation, which is the rate-limiting step of chromophore formation, was larger than that of either EBFP or EBFP2 (**Table 1** and **Supplementary Fig. 4c**).

Because one of the mutations caused a phenylalanine-to-serine substitution at amino acid 223, which faces the outside of the protein, it was possible that Sirius had different oligomerization properties than its ancestral protein, mseCFP. However, the fluorescence signal of Sirius expressed in HeLa cells was evenly distributed in the cytoplasm and nucleus without any visible aggregates or nonspecific localization

(**Supplementary Fig. 5a**), suggesting that it is a monomer, although this would need to be confirmed by additional analysis **[AU: OK as edited? I've added this sentence since gel filtration was not reported]**. We made fusion proteins between Sirius and several proteins, and confirmed that the fused Sirius did not perturb their localization (**Supplementary Fig. 5b-i**); an exception is the fusion of Sirius with α-tubulin, which localized not only to microtubules but was also found in the cytoplasm (data not shown). Optimization of amino acid linker length between Sirius and α-tubulin may improve the localization.

While observing Sirius fluorescence under the microscope, we noticed that Sirius was hard to photobleach. When compared with EBFP and EBFP2 in HeLa cells, the photobleaching kinetics of Sirius using a mercury arc lamp was 62 times and 5 times slower than that of EBFP and EBFP2 (**Fig. 1h** and **Table 1**), respectively. Furthermore, although the bleaching curves of EBFPs showed exponential decay, that of Sirius exhibited two components, a flat, stable component followed by exponential decay, suggesting a complicated bleaching process (**Fig. 1h**). This phenomenon was never observed when used an intense 375 nm laser, in which case Sirius showed almost the same photostability as EBFP2 (**Fig. 1j** and **Table 1**). We also calculated the quantum yield for photobleaching (Φ_{bleach}), which does not depend on molar extinction coefficient (ε) of each fluorescent protein (**Table 1**) **[AU: OK as edited?]** (See supplementary methods and supplementary ref. 16 for the calculation). Φ_{bleach} of Sirius (9.79×10^{-6}) was much smaller than that of EBFP

(1.13×10^{-4}) and comparable to that of EBFP2 (5.12×10^{-6}).

The most noteworthy feature of Sirius is its fluorescence stability in a wide range of proton concentrations (pH 3 to pH 9) (**Fig. 2a**). Presumably, this is due to the Phe66 mutation of the chromophore, since the resulting benzyl, unlike phenol, has no ionizable group. This pH insensitivity of Sirius may make it highly suitable for fluorescence imaging in acidic environments, such as in phagosomes. To examine this possibility, we observed phagocytosis of FP-expressing bacteria by *Dictyostelium discoidium*. Two-photon excitation by a 780-nm pulse laser was used to minimize photodamage induced by wide-field UV excitation of the highly photosensitive *Dictyostelium* cells. Although the excitation of Sirius at 780 nm is not effective when compared with that of EBFP2 (**Fig. 2b**), it was sufficient to identify Sirius-expressing specimens. Using EGFP-expressing bacteria, the fluorescence signal disappeared before the bacteria were completely digested in phagosomes (**Fig. 2c** and **Supplementary Movie 1**, left panel). In contrast, using Sirius-expressing bacteria, we could visualize the entire process of phagocytosis (**Fig. 2c** and **Supplementary Movie 1**, right panel).

Sirius is potentially an ideal donor to pair with mseCFP, since the emission spectrum of Sirius overlaps substantially with the absorption spectrum of mseCFP (**Supplementary Fig. 6a**). However, the spectral overlap J (0.71×10^{-13} M^{-1} cm^3) is smaller than in some other FRET pairs, such as CFP-YFP (J=1.89×10^{-13} M^{-1} cm^3) due to the fourth

power wavelength dependency of J. Also, when assuming κ^2=2/3, the Förster distance (R_0) of Sirius-mseCFP pair (R_0 = 3.7 nm) is smaller than that of CFP-YFP (R_0 = 4.7 nm), the most popular FRET pair (**Supplementary table 1**) because of the lower Φ_{FL} of Sirius. However, despite these drawbacks, the Sirius-mseCFP fusion protein (joined by a Leu-Glu peptide linker) showed a moderate sensitized emission from mseCFP (**Supplementary Fig. 6b**), with 43% FRET efficiency (**Supplementary Fig. 6c** and **Supplementary Note 1**). Encouraged by this result, we constructed an indicator for caspase-3 activation[4] by fusing the caspase-3 substrate Asp-Glu-Val-Asp between Sirius and mseCFP, yielding SC-SCAT3. We then monitored the change in FRET signal of SC-SCAT3 in apoptotic HeLa cells. As shown previously[5], we could visualize caspase-3 activation initiated first in the cytoplasm and then in the nucleus, and which was followed by cell shrinking (see below).

Recently, multiple-FRET imaging by using two independently-excitable FRET pairs was reported[6]. Because the donors of the FRET pairs have distinct excitation profiles, there was only slight cross-excitation, allowing an accurate ratiometric measurement of the two FRET indicators. We have expanded the dual FRET imaging arsenal with a different strategy that makes use of two FRET pairs, Sirius-mseCFP and Sapphire-DsRed (**Supplementary Fig. 6d**), both of which can be excited with a single wavelength (380 nm, or 720 nm by two-photon excitation) (**Supplementary Fig. 6e**). In combination with linear spectral unmixing[7], this allows single-excitation-quadruple-emission measurements,

even if both FRET pairs are present at the same intracellular location. To verify this method, we co-expressed SC-SCAT3 and SapRC2, a Ca^{2+}-indicator based on Sapphire and DsRed[8], in HeLa cells, Upon apoptosis induction by TNF-alpha treatment, most of the Ca^{2+} oscillation was seen within the first 90 min, then ceased[9]; in contrast, caspase-3 activation was seen at around 120 minutes after apoptosis induction (**Fig. 3** and **Supplementary Movie 2**). Such dual FRET imaging should allow a variety of experiments designed to elucidate the dynamic relationships among multiple biological phenomena within a single cell.

Note: Supplementary information is available on the Nature Methods website.

ACKNOWLEDGMENTS

We thank R. E. Campbell (University of Alberta) and A. Miyawaki (RIKEN) for providing the cDNA for EBFP2 and SapRC2, respectively. This work was partly supported by Grants from Scientific Research on Advanced Medical Technology of the Ministry of Labor, Health and Welfare of Japan and the Japanese Ministry of Education, Science and Technology.

ACCESSION NUMBER

The nucleotide sequence of Sirius has been deposited in the GenBank/EMBL/DDBJ databases with the accession number AB444952.

AUTHOR CONTRIBUTIONS

W.T. performed experiments, data analysis; T.M. and I.K contributed to gene construction; T.T, T.N and K.S set-upped microscopy systems; K.H contributed to imaging of phagocytosis; T.N. contributed to the conceptual development, experimental design, data analysis and manuscript preparations.

COMPETING INTERESTS STATEMENT

The authors declare no competing financial interests.

REFERENCES

1. Cubitt, A.B. et al. Understanding, improving and using green fluorescent proteins. *Trends*. *Biochem*. *Sci*. **20**, 448-455 (1995).

2. Matsuda, T., Miyawaki, A. & Nagai, T. Direct measurement of protein dynamics inside cells using a rationally designed photoconvertible protein. *Nat*. *Methods*. **5**, 339-345 (2008).

3. Nagai, T. et al. A variant of yellow fluorescent protein with fast and efficient maturation for cell-biological applications. *Nat*. *Biotechnol*. **20**, 28-29 (2002).

4. Xu, X. et al. Detection of programmed cell death using fluorescence energy transfer. *Nucleic*. *Acids*. *Res*. **26**, 2034-2035 (1998).

5. Takemoto, K., Nagai, T., Miyawaki, A. & Miura, M. Spatio-temporal activation of caspase revealed by indicator that is insensitive to environmental effects. *J*. *Cell*. *Biol*. **160,** 235-243 (2003).

6. Ai, H.W., Hazelwood, K.L., Davidson, M.W. & Campbell, R.E. Fluorescent protein FRET pairs for ratiometric imaging of dual biosensors. *Nat*. *Methods*. **5**, 401-403 (2008).

7. Zimmermann, T., Rietdorf, J. and Pepperkok, R. Spectral imaging and its applications in live cell microscopy. *FEBS*. **546**, 87-92 (2003).

8. Mizuno, H., Sawano, A., Eli, P., Hama, H. & Miyawaki, A. Red fluorescent protein from Discosoma as a fusion tag and a partner for fluorescence resonance energy transfer. *Biochemistry*. **40**, 2502-2510 (2001).

9. Pu, Y., Luo, K.Q. & Chang, D.C. A Ca^{2+} signal is found upstream of cytochrome c release during apoptosis in HeLa cells. *Biochem*. *Biophys*. *Res*. *Commun*. **299**, 762-769 (2002).

Figure 1. Characterization of UMFP variants. (**a**) Fluorescence of purified UMFP-1 and conventional fluorescent proteins, taken with 365-nm excitation. (**b**) Absorption (dotted lines) and emission spectra (solid lines) of UMFP-1 and EBFP. (**c-f**) Multi-color imaging of

HeLa cells labeled with UMFP1-H2B (c), mseCFP-er (d), Venus-mit (e), and mCherry-mt (f). (**g**) Merge of images in c, d, e, and f. Scale bars, 10 μm. (**h, i**) Photobleaching curves of Sirius, EBFP2, and EBFP in HeLa cells, excited by a mercury arc lamp through a 352 nm-388 nm excitation filter (**h**) and using a 375 nm diode laser (**i**). All curves are normalized to the fluorescence intensity before photobleaching. Error bars are s.d. (n=3).

Figure 2. pH sensitivity of Sirius. (**a**) The curves show pH dependence of the fluorescence emission of purified Sirius, tagRFP, mseCFP, EBFP2, and EGFP. Mean values from three independent experiments were plotted. Error bars indicate s.d. (**b**) Mean fluorescence intensity of the indicated proteins expressed in HeLa cells (n = 30), under two-photon excitation at 780 nm. Error bars indicate s.e. (**c**) Series of confocal images showing the phagocytosis of FP-expressing bacteria by *Dictyostelium discoidium* at the indicated times (in seconds). The DIC image of the cells was merged with the fluorescence image. Scale bar, 5μm.

Figure 3. Dual functional imaging with two FRET pairs. (**a**) Pseudo-colored ratio images of representative HeLa cells co-expressing SC-SCAT3 (top row) and SapRC2 (bottom row), at the indicated times (in minutes) after treatment with TNF-alpha . The colored bars represent the cyan-to-ultramarine intensity ratio (top row) or red-to-green intensity ratio (bottom row). Scale bar, 10 μm. (**b**) Time course of the fluorescence intensity, a.u, arbitrary units. (**c**) Intensity ratio of both mseCFP/Sirius (blue line) and DsRed/Sapphire (red line) after four-color spectral unmixing in the region of interest shown in a.

Table 1. Physical and optical properties of ultramarine fluorescent proteins

variants.

Name	Color	λ_{ab} (nm)	λ_{em} (nm)	ε ($M^{-1}cm^{-1}$)	Φ_{FL} [a]	p*K*a	τ_{bleach} [b] (arc lamp)	τ_{bleach} (laser)	Φ_{bleach} [c] ($\times10^{-6}$)	Relative fluorescence at 37 [d] *E. coli*	HEK293	K_{ox} ($\times10^{-4}s^{-1}$)
mseCFP	Cyan	434	474	30,000	0.4	6.4	ND	ND	ND	ND	ND	ND
mseCFP-W66F	ultramarine	355	424	14,000	0.003	ND[e]	ND	ND	ND	ND	ND	ND
UMFP-1	ultramarine	355	424	15,000	0.07	< 3.0	ND	ND	ND	ND	ND	ND
UMFP-2	ultramarine	355	425	15,000	0.11	< 3.0	ND	ND	ND	ND	ND	ND
UMFP-3	ultramarine	355	424	13,000	0.16	< 3.0	ND	ND	ND	ND	ND	ND
UMFP-4 (Sirius)	ultramarine	355	424	15,000	0.24	< 3.0	62	7.3	9.79	2.2	1	5.6
EBFP2	Blue	380	447	34,000	0.54	5.7	13	9.9	5.12	2.8	1.8	4.4
EBFP	Blue	380	448	32,000	0.25	6.3	1	1	113	1	1	4.7

[a] Fluorescence quantum yield. [b] Time needed to bleach 1/e of maximum fluorescence intensity in HeLa cells (n=3) relative to EBFP. [c] Photobleaching quantum yield. [d] Fluorescence intensity in *Escherichia coli* and HEK293 in PBS at 37℃ and adjusted OD at 600 nm and western blotting **[AU: please explain this a bit better]**, respectively. [e] ND, not determined.

Supplementary File	Title
Supplementary Figure 1	Sequence alignment of UMFP and GFP variants.
Supplementary Figure 2	Comparative characterization of the absorption and fluorescence properties of UMFP variants.
Supplementary Figure 3	Dual color imaging of UMFP-mito and EBFP-H2B in HeLa cells by linear spectral unmixing.
Supplementary Figure 4	Fluorescence emission intensity of Sirius, EBFP, and EBFP2 at 37 $_{o}$C.
Supplementary Figure 5	HeLa cells expressing Sirius or a Sirius fusion protein.
Supplementary Figure 6	Dual FRET imaging by single-excitation-quadruple-emission measurement mode.
Supplementary Table 1	Förster radius (nm) of the fluorescent protein pairs.
Supplementary Note 1	Photobleaching of CFP.
Supplementary Note 2	Linear unmixing of dual FRET measurement.
Supplementary Video 1	Imaging the phagocytosis of bacteria by *Dictyostelium discoidium*. Tracking of bacteria expressing EGFP (green color in left panel)

	and Sirius (cyan color in right panel) phagocytosed by a *Dictyostelium* cell.
Supplementary Video 2	Dual functional imaging using two FRET-based indicators. Dual FRET ratio imaging of HeLa cells co-expressing two FRET indicators, SC-SCAT3 (left) and SapRC2 (right).
Supplementary Methods	Mutagenesis, gene construction, screening, spectroscopy, measurement of fluorescence intensity at 37 ^{o}C, protein maturation kinetics. pH titration, photostability, two-photon excitation microscopy, fluorescence intensity with two-photon excitation microscopy, FRET efficiency, quadruple-color imaging in dual FRET, and linear unmixing of fluorescence spectrum.

AOP:

A fluorescent protein, Sirius, with the most blue-shifted emission spectrum to date, is reported. Sirius allows extended multicolor imaging, as well as imaging in acidic environments due to its pH insensitivity.

Issue:

A fluorescent protein, Sirius, with the most blue-shifted emission spectrum to date, is reported. Sirius allows extended multicolor imaging, as well as imaging in acidic environments due to its pH insensitivity.

Tomosugi et al., Figure 1

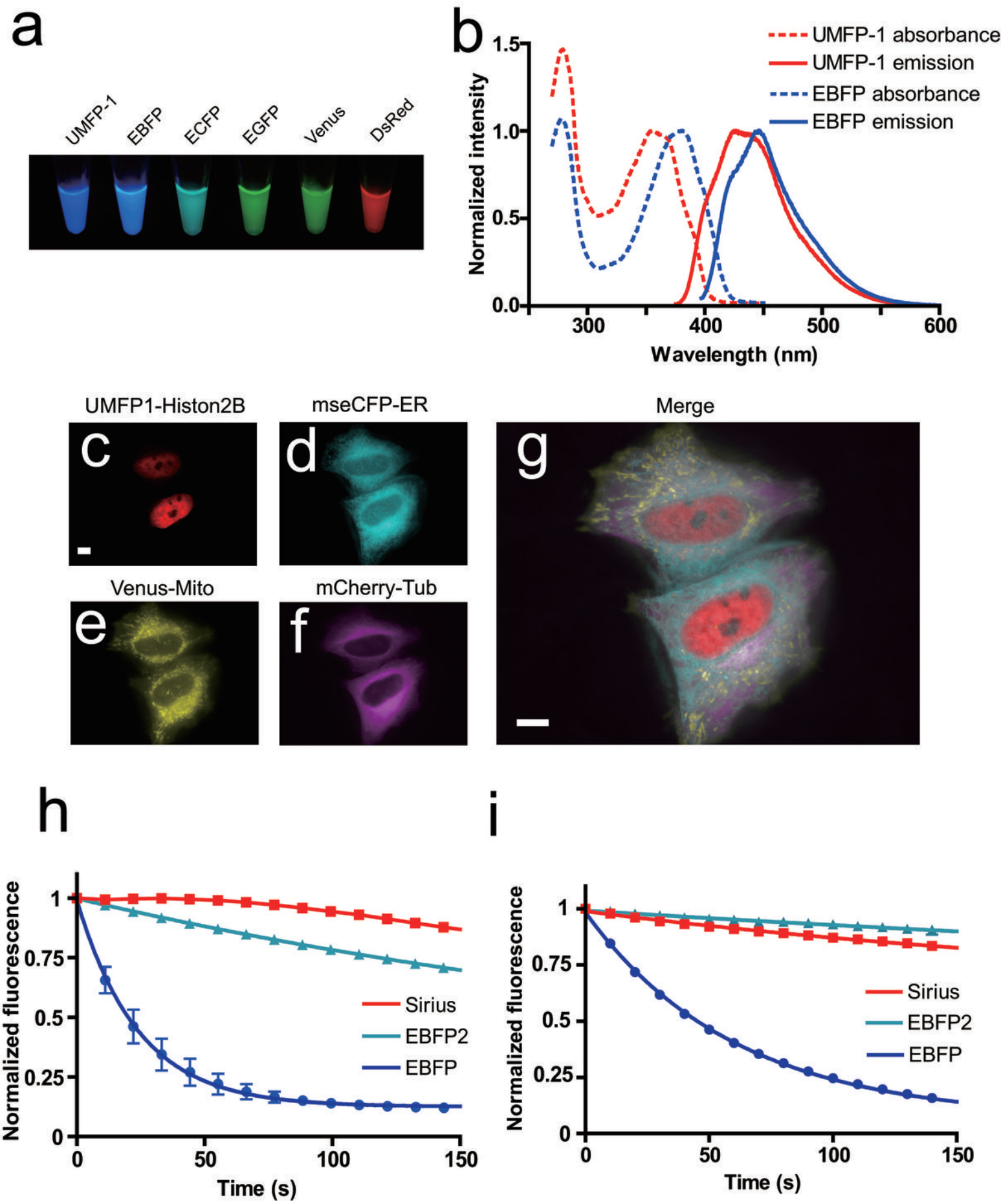

Tomosugi et al., Figure 2

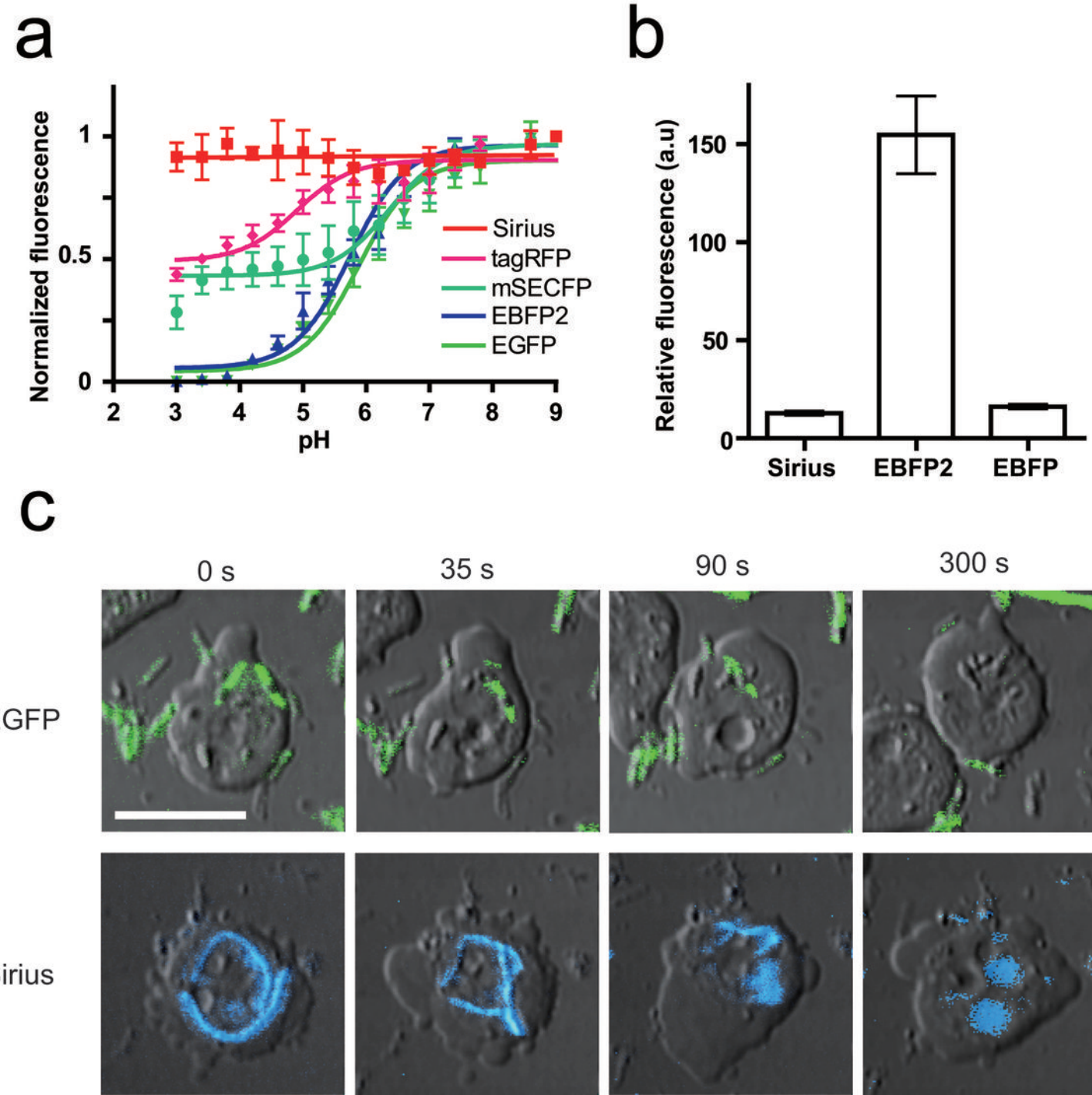

Tomosugi et al., Figure 3